JGR Planets

RESEARCH ARTICLE

10.1029/2025JE009031

Ferromagmatic Intrusions on Asteroid (16) Psyche May Be Magnetized

Samuel W. Courville[1], Hannah R. Sanderson[2], Carver J. Bierson[3], Linda T. Elkins-Tanton[4], Rona Oran[5], Joseph G. O'Rourke[1], Christopher T. Russell[6], Benjamin P. Weiss[5], and David A. Williams[1]

[1]School of Earth and Space Exploration, Arizona State University, Tempe, AZ, USA, [2]Department of Earth Sciences, University of Oxford, Oxford, UK, [3]Scottsdale Community College, Scottsdale, AZ, USA, [4]Space Sciences Laboratory, University of California, Berkeley, CA, USA, [5]Massachussets Institute of Technology, Cambridge, MA, USA, [6]University of California at Los Angeles, Los Angeles, CA, USA

Key Points:

- Sulfur-rich ferromagmatic intrusions on or near (16) Psyche's surface may record remanent magnetization from a dynamo
- The Psyche mission's magnetometer could detect ferromagmatic intrusions that were >1 km wide
- Ferrovolcanism likely requires inward core solidification with an Fe-S core composition on the Fe-rich side of the Fe-FeS eutectic

Correspondence to:

S. W. Courville,
swcourvi@asu.edu

Citation:

Courville, S. W., Sanderson, H. R., Bierson, C. J., Elkins-Tanton, L. T., Oran, R., O'Rourke, J. G., et al. (2025). Ferromagmatic intrusions on asteroid (16) Psyche may be magnetized. *Journal of Geophysical Research: Planets*, *130*, e2025JE009031. https://doi.org/10.1029/2025JE009031

Received 1 MAR 2025
Accepted 29 JUN 2025

Author Contributions:

Conceptualization: Samuel W. Courville, Carver J. Bierson, Linda T. Elkins-Tanton, Joseph G. O'Rourke
Investigation: Samuel W. Courville
Methodology: Samuel W. Courville, Hannah R. Sanderson
Software: Samuel W. Courville, Hannah R. Sanderson
Writing – original draft: Samuel W. Courville
Writing – review & editing: Samuel W. Courville, Hannah R. Sanderson, Carver J. Bierson, Linda T. Elkins-Tanton, Rona Oran, Joseph G. O'Rourke, Christopher T. Russell, Benjamin P. Weiss, David A. Williams

Abstract NASA's Psyche mission will arrive at the metal-rich asteroid (16) Psyche in 2029. The mission will test whether (16) Psyche is a remnant of a melted, differentiated planetesimal that formed a molten iron metallic core. Previous studies have suggested that a molten metallic core fluid could erupt volcanically, explaining the high metal content of (16) Psyche's surface. Here we describe an origin story for (16) Psyche using thermal and compositional evolution modeling that outlines when ferrovolcanism could occur. We highlight how Psyche's Magnetometer could detect remanent magnetization associated with mantle intrusions of the core metal.

Plain Language Summary NASA's Psyche mission will reach the asteroid Psyche in 2029 to study its origins. Scientists think Psyche might be the leftover metal core of an early planetesimal, a small building block of planets. For this to be true, Psyche's interior must have once been hot enough to melt iron and form a liquid metal core. Some researchers believe that molten metal from this core could have erupted onto the surface, explaining why the asteroid's surface looks metallic from telescopic observations. This study uses computer models to explore how and when such metal eruptions, called "ferrovolcanism," might have happened. The Psyche spacecraft's instrument for measuring magnetic fields could provide evidence for these eruptions by detecting ancient magnetic fields created during the process.

1. Introduction

When it arrives in 2029, NASA's Psyche mission will become the first spacecraft to orbit a metal-rich asteroid (Dibb et al., 2024). Among other objectives, the mission will test whether the asteroid (16) Psyche is a remnant of a differentiated planetesimal that melted iron to form a molten metallic core (Elkins-Tanton et al., 2022). If (16) Psyche is the remnant of a differentiated planetesimal, then the mission could be the first to directly explore a metallic core, a region that is locked away deep beneath rocky mantles on larger planetary bodies such as Earth. One under-investigated aspect of planetesimal core formation is how a core's composition would evolve as it solidifies and how this influences a body's geodynamical evolution and the generation of a dynamo magnetic field. The asteroid (16) Psyche (henceforth Psyche) provides a chance to investigate this process.

Present day telescopic observations alone cannot confirm that Psyche is a differentiated planetesimal that is intact and has not been catastrophically disrupted by impacts. The most recent estimates of the density of Psyche are approximately 4 g/cc (Elkins-Tanton et al., 2020; Farnocchia et al., 2024; Siltala & Granvik, 2021). Given that silicate achondrite meteorites have grain densities of ∼3.0 g/cc (Flynn et al., 2018), and iron has a density of ∼7.8 g/cc (Consolmagno et al., 2008), the asteroid likely includes a mix of metal and silicates (or another low-density material). The exact fraction of each component depends on Psyche's porosity (Bierson et al., 2025). A pure metal Psyche could not retain porosity if its temperature is above 800 K (Nichols-Fleming et al., 2022). Thus, any porosity in the metal component of Psyche must have been added after Psyche cooled (Nichols-Fleming et al., 2022). Thus, the density estimates cannot uniquely constrain Psyche's structure, composition, or history.

However, there is likely metal exposed on Psyche's surface. The Atacama Large Millimeter Array (ALMA) has discovered that Psyche's radar albedo and thermal inertia are spatially variable (Cambioni et al., 2022; De Kleer et al., 2021; Shepard et al., 2021). Some regions have higher radar albedos indicative of metal content, perhaps 20

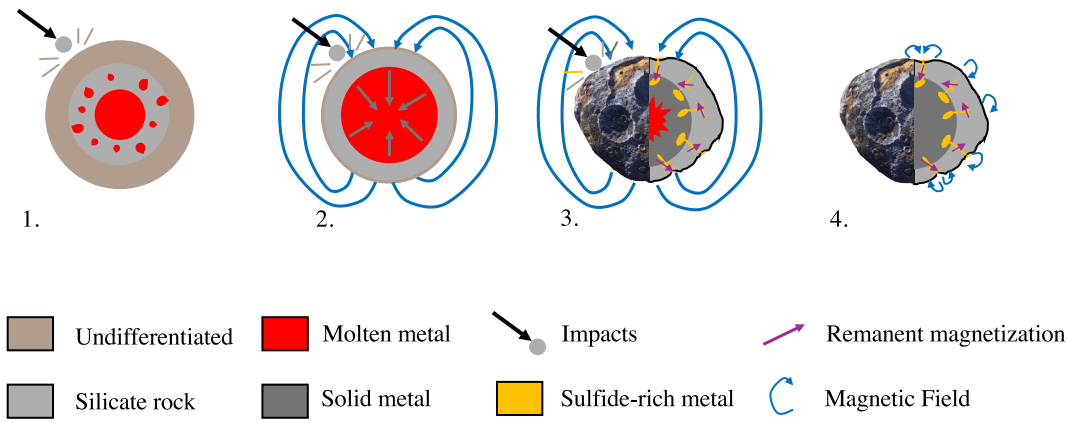

Figure 1. Cartoon depiction of the stages of evolution for a ferrovolcanic Psyche: 1. differentiation, 2. compositional dynamo generation during core solidification, 3. ferrovolcanic eruptions and recording of the dynamo field during dike cooling, and 4. Psyche's hypothetical present-day interior. We model the thermal and compositional evolution of the solidifying core. We assume that Psyche is differentiated with a metallic core overlain by a silicate mantle. Some mantle stripping is necessary to explain Psyche's density. For discussion of how impacts may alter this evolution, see Section 5.4.

wt. % or more over horizontal scales of tens of kilometers (Cambioni et al., 2022). How these metal-rich regions formed is unclear. Impacts could have exposed the core metal and perhaps distributed it across the surface. However, in that case, metal should be associated with depressions. There is no strong correlation between large basins and metal (Cambioni et al., 2022). Another alternative is ferrovolcanism (the eruption of core metal onto Psyche's surface) or impact exposed ferromagmatism (the intrusion of core fluid into the Psyche's overlying mantle or crust). This hypothesis is consistent with observations of Psyche's density and patches of metal at the surface (Abrahams & Nimmo, 2019; Johnson et al., 2020).

Ferrovolcanism is a hypothetical process that could occur on bodies with solidifying cores (Abrahams & Nimmo, 2019; Johnson et al., 2020). As the core solidifies, sulfur-rich molten fluid intrudes into the mantle, possibly reaching the surface (Johnson et al., 2020). Given a chondritic bulk composition, Psyche's likely core composition would be rich in sulfur (~>10 wt. %, Bercovici et al., 2022). Omitting other elements and assuming an idealized Fe-S composition, as the molten core liquid solidifies, it enriches in S from fractional solidification of Fe. The more the fluid is enriched in S, the less dense it would be relative to solidified Fe and thus the more buoyant it would be. The fluid's increased buoyancy could force melt intrusions to the surface. At any point during this series of events, impacts could have disrupted Psyche. Though we do not model impact processes, impacts are likely required to explain Psyche's present-day shape, its high obliquity (Shepard et al., 2021), and its elevated density by some degree of mantle stripping of less dense material.

Magnetometry investigations may be the best way to identify the signatures of ferromagmatic intrusions. Psyche has many large impact basins (Shepard et al., 2021). Although the impacts may reveal information about Psyche's interior (Caldwell et al., 2020; Clenet et al., 2014; Ermakov et al., 2014), impacts may have also erased any geomorphic evidence of surface processes in Psyche's early history, for example, Vesta (D. A. Williams et al., 2014). Furthermore, molten core metal intruding into a cold mantle may solidify before reaching the surface. We posit that if the core had an active dynamo during solidification (H. R. Sanderson et al., 2024), then these metallic dikes could have acquired remanent magnetization. Figure 1 displays a conceptual model for how ferrovolcanism would occur in Psyche. First, Psyche accretes a chondrite-like composition and subsequently differentiates. As Psyche cools, its core could solidify from the outside inward (Scheinberg et al., 2016) and generate a dynamo. Intrusions of the molten core fluid (i.e., ferromagmatic dikes) could acquire remanent magnetization from the core dynamo as they solidify.

Despite past studies suggesting that ferrovolcanism could explain Psyche's surface, no one has yet evaluated whether Psyche's thermal history and molten core evolution would support ferromagmatism that leads to ferrovolcanism. Additionally, the hypothesis has not been evaluated for detectability with magnetic methods. Here, we place ferrovolcanism in the context of Psyche's thermal and magnetic field generation history using thermal evolution models, and we evaluate the potential for detecting a remanent field with the Magnetometer on the

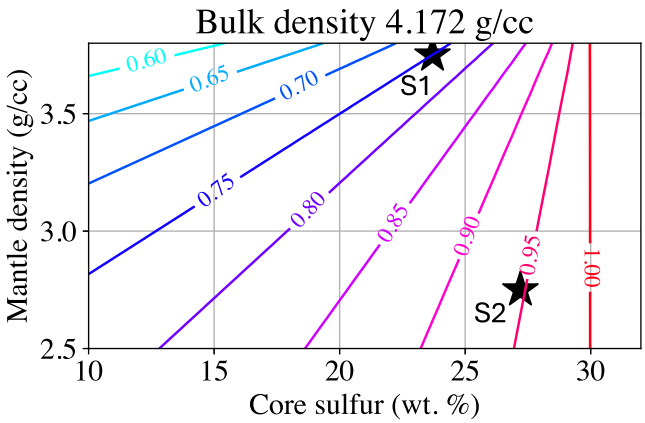

Figure 2. Contours of Psyche's core radius fraction as a function of mantle density and core sulfur content assuming a bulk density of 4.172 g/cc (Farnocchia et al., 2024). If Psyche has a metallic core, then there are a range of plausible core sizes depending on Psyche's bulk density and the density of the silicate mantle and metallic core. The black stars represent the two scenarios (thick mantle—S1; thin mantle—S2) that we explore in this paper.

Psyche spacecraft (Weiss et al., 2023). First, we present two thermal evolution models consistent with Psyche's bulk density: a thick and thin mantle. Next, we evaluate whether ferromagmatic intrusions could reach the surface, and whether they could acquire detectable remanent magnetization upon cooling. Finally, we discuss the limitations, and unknown factors inherent in ferrovolcanism. The goal of this article is to provide testable predictions for ferrovolcanism so that when the Psyche mission arrives at the asteroid, it is possible to deduce aspects of Psyche's core history through the detection or absence of ferrovolcanism.

2. Methods

We assess whether detectable remanent magnetization from ferromagmatism on Psyche could be detected in three steps. First, we model the thermal evolution and magnetic field generation history of Psyche. This determines when the dynamo was active and the thermal state of the mantle when ferromagmatic dikes had intruded. Second, we calculate the possible height that dike intrusions could reach into the mantle. Third, we determine the possible magnetization recorded by the dikes and combine this with the dike sizes to predict the observable field strength at the surface.

2.1. Psyche's Composition and Internal Structure

The most recent estimate of Psyche's density is 4.172 ± 0.145 g/cc (Farnocchia et al., 2024). Assuming Psyche has a differentiated interior, made of a silicate mantle overlying a metal core, then the size of the core depends on the core and mantle densities (Bierson et al., 2025, Kim & Hirabayashi, 2022). If Psyche accreted an ordinary or carbonaceous chondrite-like composition, then Psyche's current density requires that impacts strip away some, but not all, of the silicate mantle after differentiation. Thus, we choose to model two partially-stripped-mantle cases for Psyche: scenario 1, a thin 6 km mantle; and scenario 2, a thick 30 km mantle (Figure 2). In both cases, we assume that the core consists only of iron and sulfur. We neglect nickel and other light elements in this model, though we discuss their implications in Section 4.1. If Psyche was formed from chondritic precursor material, the primordial core composition may have ranged between ∼10 and 30 wt. % sulfur, with lower values corresponding to ordinary chondrites and higher values for carbonaceous chondrites (Bercovici et al., 2022). Although our thick and thin mantle models assume a spherical Psyche, such cases could also potentially be consistent with different areas of Psyche. For example, if Psyche's core is more spherical than its current triaxial ellipsoid surface, then the depth to the core at Psyche's poles would be less than at the equator (Bierson et al., 2025, Kim & Hirabayashi, 2022).

2.2. Thermal Modeling

For ferromagmatic dikes on Psyche to be magnetized by Psyche's dynamo magnetic field, two criteria must be satisfied. First, Psyche must have generated a magnetic field during the intrusion of the molten core fluid. Second, the dikes must have cooled below the blocking temperature of magnetic carriers while the dynamo was active. The cooling rate of the dikes depends on the mantle temperature and hence, Psyche's overall thermal evolution. We calculate Psyche's thermal evolution and predict its dynamo generation periods using an existing model (H. R. Sanderson et al., 2025). Table 1 lists the properties we assume for the two modeled cases, with all other parameter values taken from H. R. Sanderson et al. (2025).

Table 1
Model Input Values for Scenarios 1 and 2

Parameter	Symbol	Value—Scenario 1	Value—Scenario 2
Radius	r	120 km	120 km
Mantle density	ρ_m	3.75 g/cc	2.75 g/cc
Core radius	r_c	90 km $\left(\frac{r_c}{r} = 0.75\right)$	114 km $\left(\frac{r_c}{r} = 0.95\right)$
Initial core sulfur	X_S	23.7 wt. %	27.2 wt. %

Note. All other parameter values are the same as Table 1 in H. R. Sanderson et al. (2025).

The model begins with instantaneous accretion of an undifferentiated planetesimal consisting of a mixture of metal and silicates. The planetesimal is heated by ^{26}Al and ^{60}Fe and both metallic and silicate phases begin to melt. Differentiation occurs when the body reaches the critical melt fraction. The critical melt fraction is the volume fraction of material that must melt for the undifferentiated material to become rheologically weak, allowing dense metal droplets to sink into the center of the planetesimal. We assume a value of 0.5

to explore a wide range of initial core S contents (H. R. Sanderson et al., 2025). After differentiation, proto-Psyche consists of two layers: an Fe-S core and an overlying silicate mantle. Then, ^{26}Al and ^{60}Fe partition into the mantle and core, respectively. We assume that the surface temperature is 200 K, consistent with temperatures at Psyche's location in the asteroid belt. Heat transfer in each layer occurs by convection or conduction. The mantle convects in the stagnant-lid regime, which consists of an isothermal interior and stagnant, conductive boundary layers at the surface and core-mantle boundary (CMB). These conductive boundary layers thicken (at different rates) as the mantle cools, and convection ceases when the combined boundary layer thickness equals the thickness of the mantle (H. R. Sanderson et al., 2025). The core convects whenever the heat flux out of the core is positive; the adiabatic gradient is neglected due to the low gravitational acceleration in planetesimal cores (H. R. Sanderson et al., 2025).

The model assumes that the core contains only iron and sulfur. The Fe-FeS liquidus controls the evolution of sulfur in the core. As the core solidifies, we assume that all sulfur remains in the liquid core, thereby increasing the sulfur fraction and lowering the crystallization temperature (Buono & Walker, 2011; Goldstein et al., 2009). Dendritic inward core solidification could trap pockets of melt and thus prevent all the sulfur from remaining in the core, but we assume this fraction is small and negligible compared to the volume of the core (See Section 4.4). To ensure that the core is molten at the beginning of the thermal evolution, the minimum initial core sulfur content that can be used in the model is the intersection between the planetesimal's differentiation temperature (temperature at the critical melt fraction) and the Fe-FeS liquidus. This corresponds to 23.4 wt. % in scenario 1 and 23.0 wt. % in scenario 2.

2.3. Dynamo Modeling

A molten core in a planetesimal may produce a magnetic field through dynamo action if fluid convection is sufficiently vigorous in the core. The vigor of core flow is measured by the dimensionless magnetic Reynold's number, Re_m,

$$Re_m = \frac{ul}{\lambda}, \tag{1}$$

where u and l are the characteristic speed and length scale of convection, respectively, and λ is the magnetic diffusivity (H. R. Sanderson et al., 2025). If Re_m exceeds a critical value, a dynamo can be generated. We assume a critical Re_m of 10, which has previously been demonstrated to be the appropriate critical value for planetesimals (H. R. Sanderson et al., 2025).

In planetesimals, core flows can be driven by thermal or compositional convection. In thermal convection, rapid core cooling destabilizes the core, as the top of the core becomes cooler and denser than the center (Nimmo, 2007). Compositional convection occurs due to compositional density differences arising from core solidification as the remaining molten core becomes enriched in light elements as the core solidifies (Gubbins, 1977; Nimmo, 2007). The buoyancy flux from either (or both) of these types of convection can be used to calculate the convective speed and magnetic field strength. We use an existing model that evaluates both thermal and compositional dynamos (H. R. Sanderson et al., 2025).

2.4. Dike Intrusion Modeling

Planetesimal cores may solidify inwardly due to the low pressure at their CMBs (Dodds et al., 2025; Q. Williams, 2009, 2025). For an Fe-S core on the Fe-rich side of the Fe-FeS eutectic (~<31 wt. % S), pure iron solidifies first and the remaining liquid becomes progressively more enriched in sulfur. Thus, a less dense, sulfur-rich liquid may become trapped beneath a denser, solidified iron layer at the top of the core (Johnson et al., 2020). The buoyancy force of an S-rich core liquid trapped within solid iron may drive intrusions of the fluid into the mantle above.

The density of the trapped Fe-S liquid is intermediate between the bulk Fe-S core and the silicate mantle. Therefore, assuming hydrostaticity, the buoyancy-driven intrusion of a ferromagmatic dike may therefore be thought of as an iceberg: to support a given height of sulfur-rich melt intruding into the mantle, there must be a commensurate amount of underlying melt in the core (see Figure 3). The intrusion's height depends on the level of neutral buoyancy,

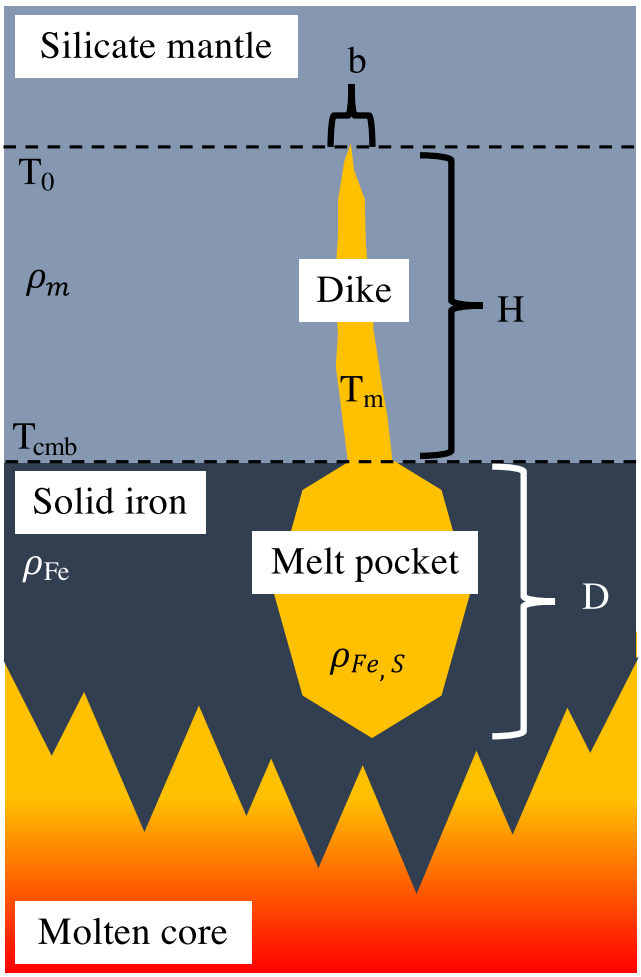

Figure 3. If the inward, dendritic solidification of the core traps a pocket of core fluid, the trapped fluid experiences a buoyancy force that may lead to a ferromagmatic intrusion. The height that the fluid can intrude is a function of the pocket's depth and the densities of the fluid, the mantle, and the solidified core (see Equation 2). Once a dike intrudes into the mantle, the timescale over which the dike would solidify is a function of the mantle's background temperature relative to the melt's temperature, T_m. The dike would cool fastest at its maximum extant where the mantle would have a lower temperature, denoted T_0 (see Equations 4 and 5).

$$H = \frac{D(\rho_{\mathrm{Fe}} - \rho_{\mathrm{FeS}})}{\rho_{\mathrm{FeS}} - \rho_M}, \tag{2}$$

where D is the depth of the melt pocket in the core, and ρ_M is the density of the mantle (Johnson et al., 2020). The maximum value of H at any given time is limited by the thickness of the solidified core. For the density of the Fe-S fluid, we use (Morard et al., 2018),

$$\rho = \left(-3108\, {X_{S,\mathrm{at}}}^2 - 5176 X_{S,\mathrm{at}} + 6950\right), \tag{3}$$

where $X_{S,\mathrm{at}} = \left(1 + \frac{1 - 0.01X_S}{0.01X_S}\frac{M_{r,S}}{M_{r,\mathrm{Fe}}}\right)^{-1}$ is the atom % S, X_S is the sulfur content in wt % and $M_{r,\mathrm{Fe}}$ and $M_{r,S}$ are the molar masses of iron and sulfur, respectively.

Whether or not the dikes can acquire remanent magnetization depends on how long it takes them to solidify and cool below their Curie points (see Section 2.5). We calculate the timescale of solidification of a dike, t_s, from,

$$t_s = \frac{b^2}{4\kappa\lambda^2}, \tag{4}$$

where b is the dike width, κ is its thermal diffusivity ($k_c = \kappa_c \rho_c c_{\mathrm{pc}}$) (Turcotte & Schubert, 2002), and λ is a non-dimensional variable that accounts for temperatures and the latent heat of the dike's solidification. We solve for λ numerically via the equation,

$$\frac{e^{-\lambda^2}}{\lambda(1 + \mathrm{erf}\,\lambda)} - \frac{L\sqrt{\pi}}{c_{\mathrm{pc}}(T_m - T_0)} = 0, \tag{5}$$

where L is latent heat of solidification (270 kJ kg^{-1}), T_m is the temperature of the molten dike, and T_0 is the temperature of the background silicates (Turcotte & Schubert, 2002). Here, c_{pc}, ρ_c, and k_c, are the dike's heat capacity, density, and thermal conductivity, respectively, which we assume are the same as for the core.

2.5. Magnetization Modeling

For magnetized ferromagmatic dikes to be detectable by Psyche's Magnetometer, we consider that at a minimum, the magnetic field strength from a dike as measured at the spacecraft's altitude must exceed ~1 nT (Weiss et al., 2023). Likely, the magnetic field signature from a small region would need to be sampled many times to determine how the field is embedded in the solar wind. The magnetic field strength of a dike depends on its size and magnetization strength. We estimate the potential present-day magnetic field from a magnetized dike assuming that it is a rectangular prism with a variable width between 0.1 and 10 km, a variable height between 0 and 25 km (constrained by Figure 5), and a length of 20 km. The field strength from a rectangular prism is available from Equation 9.19 of Blakely (1996). We assume a magnetization strength of 10^{-3} A m^2 kg^{-1}, which is consistent with uniform magnetization observed in iron meteorites, chondrites, and theoretical studies of planetesimal magnetization (Clavé et al., 2020; Cournede et al., 2015; S. W. Courville et al., 2022; Maurel et al., 2025). However, NRM in various meteorite hand samples ranges between 10^{-4} and 10^{-2} A m^2 kg^{-1} (Weiss et al., 2023).

To estimate the magnetization strength for the ferromagmatic dikes, we must make assumptions about the magnetic carriers within the dikes and their density. Although our thermal and compositional models assume a simplified Fe-S core composition, planetesimal cores also contain other elements. Under reducing conditions low

pressure Fe-S cores crystallize the ferromagnetic mineral kamacite (α-Fe which has ~1053 K Curie point). However, the inclusion of Ni and C would allow the formation of other ferromagnetic phases (e.g., Fleet, 2006; Nichols et al., 2021): martensite (α_2-$Fe_{1-x}Ni_x$ for $x \sim > 0.04$; ~1000 K Curie point), taenite (γ-$Fe_{1-x}Ni_x$ for $0.2 \sim > x \sim > 0.5$; 273–723 K Curie point), and tetrataenite (γ"-$Fe_{0.5}Ni_{0.5}$; ~593 K ordering temperature). The lower Curie and ordering temperatures of some Ni bearing phases mean that these minerals would not lock in their magnetic records until much lower temperatures, lessening their ability to record the earliest period of dynamo activity or remanence in Psyche's deeper mantle. Because ferromagmatic dikes are composed of sulfur-rich iron melt surrounded by silicates, potential magnetic carriers might also include pyrrhotite ($Fe_{1-x}S$, $x \sim 0$–0.2) and magnetite (Fe_3O_4) within silicates near or entrained in the dike. Such minerals are known to preserve remanent signatures in some chondrites (Cournede et al., 2015; S. W. Courville et al., 2022; Fu et al., 2021; O'Brien et al., 2020). Thus, there are many plausible magnetic carriers and Curie temperatures.

Sufficiently large crystals of metals, for example, kamacite or pyrrhotite, may form multidomain grains (Tauxe, 2010). Multidomain grains typically have lower magnetic coercivity than single-domain grains (Berndt et al., 2018; Tauxe, 2010), and therefore, they may not be able to retain all of their original magnetization over the 4 billion years between Psyche's dynamo being active and the arrival of the Psyche spacecraft. Perhaps only single-domain or pseudo-single-domain carriers in the ferrovolcanic dike are likely to retain their remanent magnetization and be detectable by a magnetometer. Iron grains encased within silicates are possible candidates for these carriers. Such inclusions have been shown to record a magnetization in the metal-rich pallasite meteorites (Tarduno et al., 2012), although the fidelity of these records is uncertain (Nichols et al., 2021). Thus, the magnetic carriers associated with a dike may belong to mantle related minerals entrained within or adjacent to the melt, and it is not a guarantee that metal intrusions could record remanent magnetization. Regardless, iron meteorites retain remanent magnetization on the meter scale (Clavé et al., 2020; Maurel et al., 2019), so ferromagmatic features likely could.

3. Results

3.1. Thermal and Dynamo Modeling Results

Both the thin and thick mantle models show periods of sulfur enrichment during core solidification, where fractional solidification gradually increases the core's sulfur content (Figure 4). After reaching the eutectic, the crystallization temperature is constant and thus core solidification proceeds more quickly. Core solidification is faster in the proto-Psyche with a larger core fraction (scenario 2) because there is a thinner silicate layer insulating the core from cooling. Dynamo generation occurs during core solidification by compositional buoyancy in both scenarios. The surface magnetic field in scenario 2 is stronger than in scenario 1 because: (a) the ratio of the core radius to mantle thickness is greater, meaning the field generation is closer to the surface and there is less decay of the field from geometric spreading; (b) the mantle is thinner, so core solidification occurs more quickly, leading to a greater buoyancy flux. Faster core cooling in scenario 2 also reduces the duration of the dynamo.

3.2. Dike Intrusion Results

We find that both scenarios allow dikes to intrude into the mantle and cool sufficiently to record a magnetization approximately halfway through core solidification (Figure 5). The dike solidification and cooling timescale ranges from ~1 kyr to ~10 Myr after formation depending on the width of the dike. The potential magnetized height of a dike is the distance between the maximum height of the dike and the temperature contour of a given Curie point. The thick crust (30 km) model in scenario 1 could produce magnetized dikes with heights up to ~23 km, whereas the thin crust (6 km) model in scenario 2 could produce magnetized dikes with heights of <5 km.

3.3. Dike Magnetization Detectability Results

We find that at the Psyche spacecraft's closest orbital altitude, Orbit D at ~75 km (Elkins-Tanton et al., 2022; Weiss et al., 2023; Zuber et al., 2022), magnetic regions associated with dikes could be detectable if their effective magnetized widths are ≥~1 km (Figure 6). The effective magnetized width associated with a dike is not necessarily the same as the dike itself. The effective magnetized region could be greater than the width of a dike because surrounding minerals can be magnetized as they are heated and cooled after intrusion (Annen, 2017; Jaeger, 1964). Additionally, if dikes occur in swarms—as is common on Earth (Ferreira et al., 2023)—then the

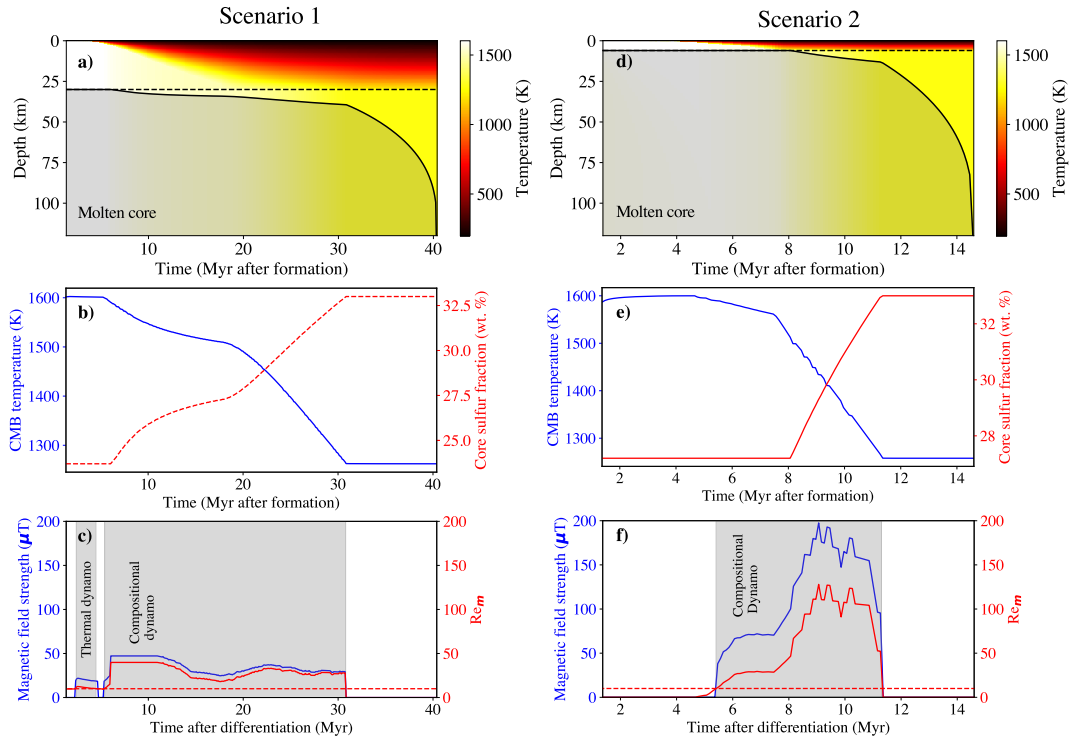

Figure 4. Psyche's thermal and dynamo evolution for scenarios 1 (left plots) and 2 (right plots). Corresponding parameter values are in Table 1. In scenario 1, the thermal model (a) shows core solidification beginning at ∼6 Myr after Psyche's formation. Sulfur enrichment of the core fluid occurs between ∼5 and 15 Myr after formation (b). A magnetic field with a strength of up to 50 μT at the surface occurs until ∼31 Myr after formation (c). A distinct thermal convection dynamo occurs before the onset of the compositional convection dynamo when sulfur enrichment occurs. In scenario 2, core solidification begins at ∼8 Myrs (a) and sulfur enrichment occurs between ∼8 and ∼11.5 Myr after formation (e). A magnetic field with a strength of up to 200 μT at the surface occurs until ∼11.5 Myr after formation (f). We estimate the magnetic field strengths and magnetic Reynolds numbers using moving averages over 1 Myr-long periods between 1 and 10 Myr after formation and over 5 Myr-long periods beyond 10 Myr after formation to damp unrealistic oscillations resulting from the discrete nature of the model. This averaging follows the approach of H. R. Sanderson et al. (2025), but with narrower windows for the moving average due to Psyche's short dynamo duration.

effective width of magnetization would be more representative of the width of the dike field. Thus, the effective magnetized region could be larger than the dike width. Detection may be further complicated by the interaction of the dike magnetic field with the solar wind, but such interactions should be accounted for by the magnetometry investigation processing (Weiss et al., 2023). Overall, we demonstrate that signals from sufficiently large ferromagmatic dikes or dike-regions could be detectable on the spacecraft's closest orbit to Psyche. We find that Psyche is more likely to produce magnetically detectable dikes (dikes that are >∼10 km tall and >∼1 km wide; see Figure 6) if Psyche has a thick mantle. Psyche could have generated a dynamo during core solidification, and if ferromagmatism occurred, the dikes would have cooled sufficiently quickly to record a magnetization.

4. Limitations and Unknowns Regarding Ferrovolcanism

Now that we have determined the criteria for the detection of ferromagmatism on Psyche, we discuss some factors that may limit the potential of ferromagmatism and ferrovolcanism to occur. Should the Psyche mission fail to detect any evidence of ferromagmatism or ferrovolcanism, the following reasons could explain why.

4.1. Immiscible Fluids

The model we describe assumes a simplified molten core composition that contains only iron and sulfur (Johnson et al., 2020). In this model, the core must approach the iron-sulfur eutectic from the sulfur-poor side, meaning that the core solidifies pure iron, and the density of the remaining molten fluid decreases relative to the solidified metal (case a, Figure 7). Eruptions occur because of the density contrast between the solidified iron and the molten

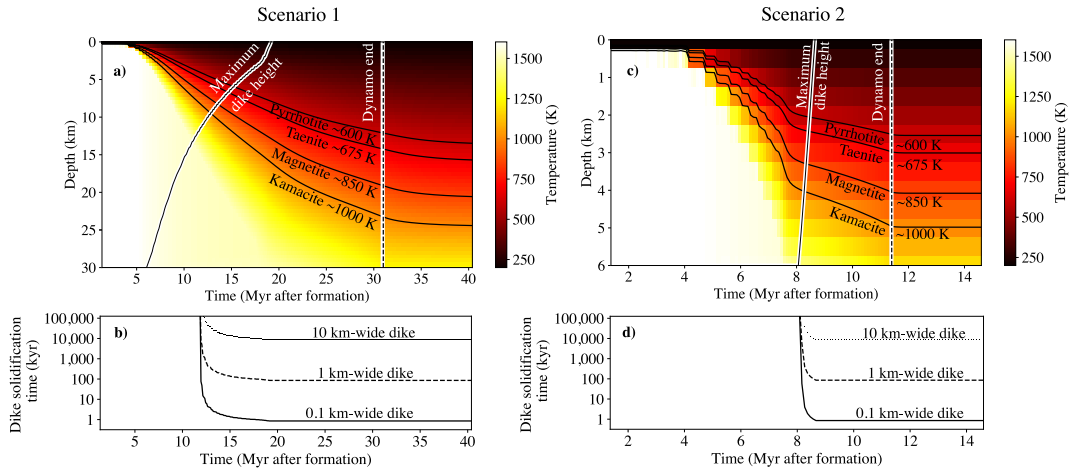

Figure 5. Maximum dike heights and dike cooling times for two scenarios: a thick mantle (left) and a thin mantle (right). The maximum possible dike intrusion height increases as the density contrast between the sulfur-enriching core and overlying solid iron increases and as the depth of the molten core beneath solidified iron increases. For scenario 1 (a), the maximum dike intrusion height reaches the surface at ∼20 Myr after formation, well before the dynamo ceases. The temperature contours correspond roughly to the Curie points of pyrrhotite (∼600 K), taenite (∼675 K), magnetite (∼850 K), and kamacite (∼1000 K). Dikes that intrude into regions above those contours could cool and acquire remanent magnetization. Panel (b) illustrates the timescale for the dike to cool to 1000 K at its maximum height. As an intrusion reaches upward, it cools more quickly. Based on the temperature profile in the mantle, dike intrusions up to ∼23 km high could acquire magnetization in scenario 1. For scenario 2, dikes may reach the surface at ∼9 Myr after formation (c), and dikes ∼1 km wide could cool before the dynamo ceases. The maximum height of intrusions with remanent magnetization could only be <5 km in scenario 2.

buoyant Fe-S. We note that the inclusion of nickel would serve to increase the core's density (Watanabe et al., 2016). Furthermore, the volume of trapped melt would expand as it solidifies, contributing to excess pressure in addition to the buoyancy. Although overall core solidification is expected to be a contraction process (Watters et al., 2004), Equation 3 suggests that as an Fe-S melt enriches in S, its volume would increase. However, at low S content, this volume increase is offset by the volume reduction from solidifying Fe. As the core enriches in S, the volume increase of the remaining melt outpaces the volume reduction of Fe crystallization (case a, Figure 7). So, a late-stage pocket of melt may experience expansion. However, an Fe-S fluid is a simplification of Psyche's likely initial bulk core composition. If a planetesimal formed from the same bulk compositions as chondrites, then the core composition after differentiation would include other light elements, such as P, Si, and C, in addition to S (Bercovici et al., 2022). When these elements are present, an immiscibility gap exists in the molten core's phase space (Morard & Katsura, 2010; Ulff-Moller, 1998). Figure 7 displays an example of the Fe-S-P system (Raghavan, 1987).

If the core's composition begins within the immiscibility gap, then there would be two separate liquids with different compositions upon differentiation and core formation. In the specific case of an Fe-S-P fluid (Chabot & Drake, 2000; Ulff-Moller, 1998), there would be a sulfide-rich fluid, which may be at or beyond the iron-sulfur eutectic, and a second fluid that would be predominantly iron with some phosphide. The sulfide-rich fluid would have a lower density, so it would rise to the top of the core and begin to solidify first. If this fluid is on the sulfur-rich side of the Fe-S eutectic point, then it would solidify troilite. The density of the remaining sulfide-rich fluid with respect to troilite would not be as conducive to ferromagmatic intrusions as the density contrast is not as significant (case b, Figure 7).

Alternatively, the core composition may begin outside of an immiscibility gap; for example, light elements could escape before or during differentiation (Hirschmann et al., 2022). In this case, the core could move into an immiscibility gap as it solidifies, which would yield a complicated relationship between the core's composition and its eruptive potential. Once the composition has moved into the immiscibility gap, the less dense immiscible fluid may experience a buoyancy force, but the density contrast and volume increase would not be as great as if there were no immiscibility (case c, Figure 7). Thus, ferromagmatism may be more likely to occur for a core

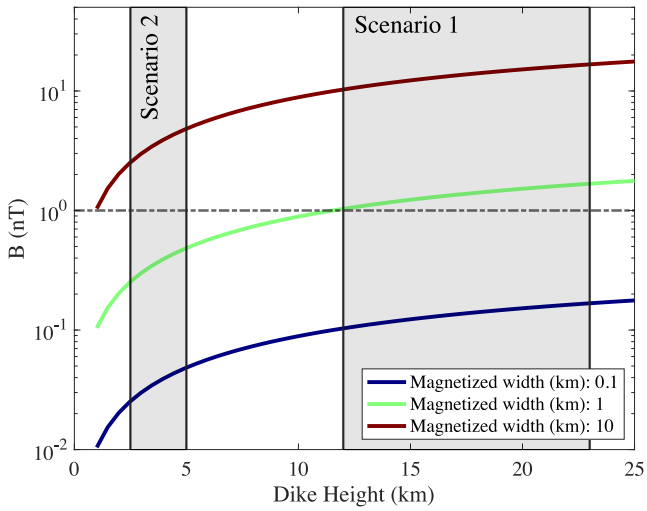

Figure 6. The strength of the magnetic field at Psyche's closest orbital distance (75 km) from a magnetized dike depends on the width of the magnetized region associated with the dike, and how high the dike intrudes into the mantle. The effective width of the magnetized region (either from one dike or a group of closely spaced dikes) needs to exceed ~1 km with a height exceeding ~10 km for the magnetization to be detectable by Psyche's magnetometer (dashed gray line), a scenario that is possible if Psyche has a thick mantle. This plot assumes an NRM intensity of 10^{-3} A m^2 kg^{-1}. A stronger or weaker magnetization would raise or lower these lines proportionally, and thus, intensities below ~10^{-4} A m^2 kg^{-1} may not be detectable at all.

composition that remains outside the immiscibility gap. Future studies should model a compositional system (e.g., Chabot & Zhang, 2022; Malvin et al., 1986) with immiscible core fluids coupled with a geodynamic model.

4.2. Fracturing and Vertical Fluid Migration

For buoyant or pressurized core fluid to erupt, it must be able to travel upward, for example, through fractures in the overlying solidified iron and silicate mantle. However, fractures may not form in the solidified iron atop the core; it is comparatively easy to fracture cold brittle silicates as opposed to warm ductile metal. Abrahams and Nimmo (2019) argue that impacts are necessary to generate the strain rates and stress required to initiate a fracture in a ductile metal crust. Impacts may also produce favorable pressure gradients and fractures to allow upward fluid migration in the mantle (Abrahams & Nimmo, 2019).

Regardless of how the fluid escapes the overlying solidified iron, it must then propagate upward through the silicate mantle. Molten Fe-S fluid is significantly denser than the silicate mantle, which differs from conventional volcanism, where melt is typically buoyant all the way to the surface (Wilson & Keil, 2012). Ferrovolcanism, thus, requires excess pressure to force the iron upward through fractures in the mantle. Cryovolcanism (Fagents et al., 2022), the volcanism that made lunar mare basalts (Zhang et al., 2023), and some volcanism driven by exsolution (Brookfield et al., 2023) demonstrate that buoyancy is not strictly necessary to drive eruptions. However, without excess pressure and fracture conduits in the mantle, it would be more reasonable to find sills of Fe-S lying atop the core, where they would make a stable density stratification. These sills could be akin to the interpreted laccolith of Brumalia Tholus on Vesta (Buczkowski et al., 2014). Potentially, sills could also form at depths above the CMB within the mantle, depending on local fracturing, where they would halt further upward dike propagation. Whether a sill could acquire detectable magnetization largely depends on whether it is high enough within the mantle to cool below a mineral's Curie point before the dynamo ends.

4.3. Core Solidification Mechanism

For ferromagmatism to occur and record remanent magnetization, core solidification must trap molten Fe-S near the CMB, and the molten core must generate a dynamo. Because of the low gravity in planetesimal cores, the adiabat and the liquidus intersect at the top of the core, and the core likely solidifies inwardly (Dodds et al., 2025; Q. Williams, 2009). Q. Williams (2025) highlights that the slope of the Buono and Walker (2011) liquidus is inconsistent with experimental data for pure iron across a range of pressures. However, the H. R. Sanderson et al. (2025) model focusses on cores with high sulfur contents (>23 wt %). For this range of core sulfur contents, planetesimal cores solidify top-down for both the Buono and Walker (2011) liquidus and the liquidus slope interpolated from the data in Q. Williams (2025). Regardless, there are multiple possible mechanisms of inward core solidification: viscous delamination of solid iron from the CMB (Neufeld et al., 2019), growth of dendrites (Johnson et al., 2020; Scheinberg et al., 2016), and iron snow (Breuer et al., 2015; Rückriemen et al., 2015; Scheinberg et al., 2016).

Dendritic solidification could provide a way to trap Fe-S melt pockets near the CMB that could produce ferrovolcanism. However, iron dendrites may prohibit the convection of material and the generation of a dynamo. In contrast, iron snow and viscous delamination both involve the sinking of solid iron within the core and could drive compositional convection but are less likely to trap Fe-S melt pockets at the CMB. As required in Figures 4 and 5, the core solidification mechanism must generate compositional convection to generate a dynamo during ferrovolcanism. Therefore, a specific set of core conditions—and perhaps a mix of the solidification mechanisms described—may be required to generate ferromagmatic dikes and magnetize them. The simultaneous existence of melt pockets that could produce ferrovolcanic eruptions at the same time as a core dynamo operates requires further study.

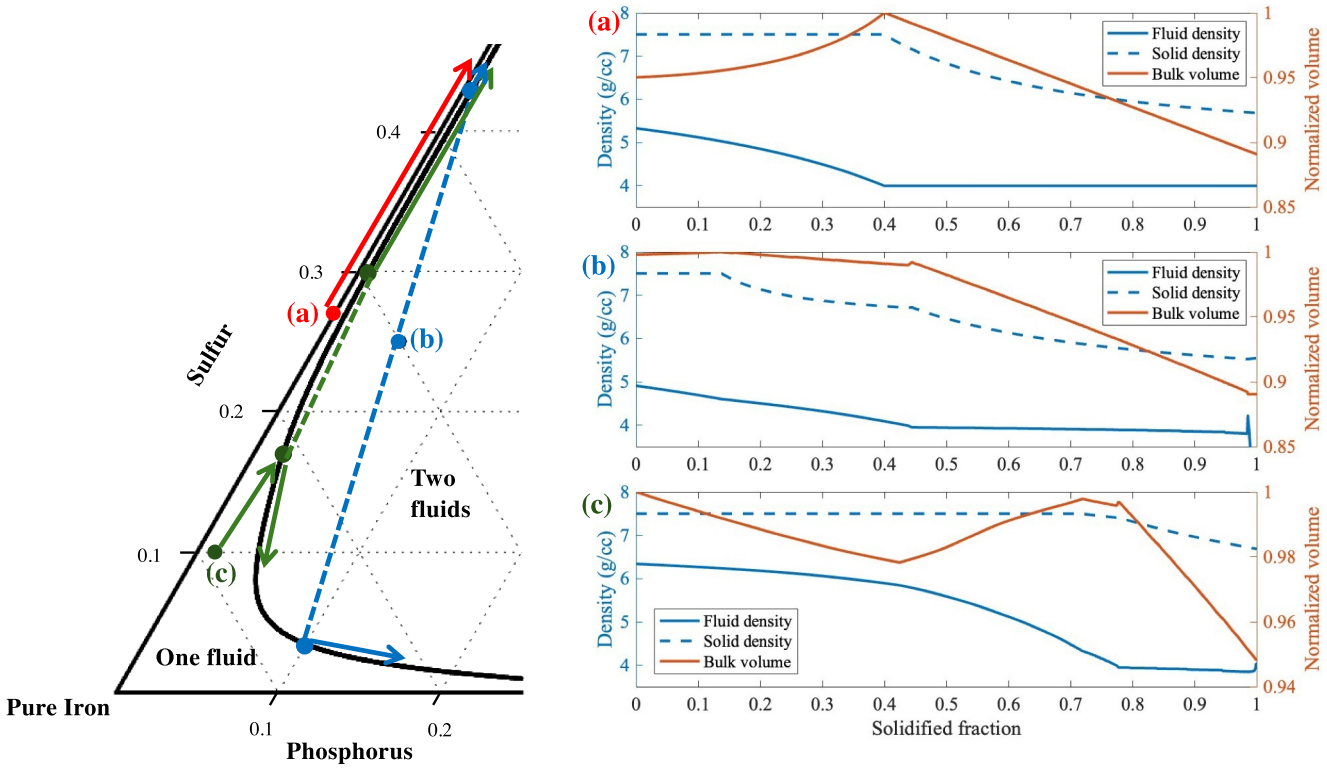

Figure 7. Left: immiscibility gap in Fe-S-P system from Raghavan (1987). Right: approximate density and volume evolution of a trapped molten core with: (a) a pure Fe-S composition that does not become immiscible, (b) a composition that is within the immiscibility gap as the pocket freezes, and (c) a pocket that starts outside the immiscibility gap but moves into it as it solidifies. Equation 3 determines the density of the fluids. The lowest density fluid in all cases would have the greatest propensity for eruption. The plot assumes that the density of solid iron is 7.8 g/cc and troilite (FeS) is 4.5 g/cc. Future work should investigate immiscible planetesimal cores with consistent equations of state that can account for all phases and their densities, for example, iron phosphides.

4.4. Intrusion Volumes

The volume of intruded material, and hence, the size of the dikes, depend on the trapped melt volume. Because the volume of trapped melt depends on the scale and geometry of potential dendrites, it is hard to place constraints on dike volumes. Conversely, dike dimensions could constrain the volume of trapped melt required. If we calculate the volume of a 1 km wide, 25 km long, 20 km high dike, and assume that the volume of the dike is approximately equal to that of the trapped melt (though it would be an evolving fraction based on the neutral buoyancy of the melt), then we find that its volume must be approximately ∼0.1% of the solidified core. Thus, if it were reasonable to assume that 10% of the solidified core volume was trapped as sulfide-rich fluid between dendrites, then the core could support ∼100 dikes of that size.

5. Discussion

5.1. Implications of Detection

If the Psyche mission finds that the density and gravity structure of asteroid Psyche is consistent with a differentiated interior, then the detection of any remanent magnetization at Psyche would imply that the body once generated a core dynamo. The remanent magnetic signature may also imply ferromagmatism. Assuming that no obvious geomorphic evidence of a ferrovolcanic flow feature is observed, then Table 2 summarizes the detections that may suggest the existence of ferromagmatism dikes.

Based on the limitations of ferrovolcanism in Section 4, there are many reasons why ferrovolcanism may not occur. Thus, the absence of ferrovolcanic features at Psyche does not yield many constraints on Psyche's formation history. Conversely, if detected, ferrovolcanism places many constraints on Psyche, such as: (a) buoyant trapped melt formed during core solidification, (b) the core solidified inwardly and dendritically, (c)

Table 2
Detection Matrix

	Localized remanent magnetization	No remanent magnetization
Detection of localized regions with sulfide-rich metal	The presence of magnetic anomalies that are spatially correlated with localized regions of sulfide-rich metal on the surface would support the ferrovolcanism model.	Ferrovolcanism may have occurred, but remanent magnetization was not recorded for one of the following reasons: - Regions of magnetization associated with dikes are too small or too weak - No dynamo activity during dike solidification, and no magnetization was acquired - Dike solidification timescale too long compared to dynamo reversal timescale - Mineralogy incompatible with remanent magnetization
No clear regions of increased metal content	Remanent magnetization may be due to subsurface ferromagmatic intrusions. However, remanent magnetization may also be due to other processes. If related to dikes, the dikes either did not reach the surface, or surface eruptions were obscured by impacts.	Ferromagmatism did not occur, or intrusive dikes did not reach the surface and did not have favorable conditions for remanent magnetization as described in the cell above

Note. The observation of remanent magnetic signatures combined with observations of sulfide-rich metal regions on Psyche's surface would be diagnostic of ferromagmatism, but the lack of either would be ambiguous.

and the mantle and outer core structure was such that it would allow fracturing (Figure 8). Furthermore, if the Psyche mission detects a remanent magnetic signature, then (d) Psyche had a core dynamo during core solidification, and (e) the stability of this dynamo field was longer than the solidification timescale of the dikes.

5.2. Measurements Complementary to Magnetometry

Besides the magnetometry investigation, other instruments onboard the Psyche spacecraft can help distinguish if the Psyche experienced ferrovolcanism. Even if there is no obvious geomorphic evidence of ferrovolcanic flows

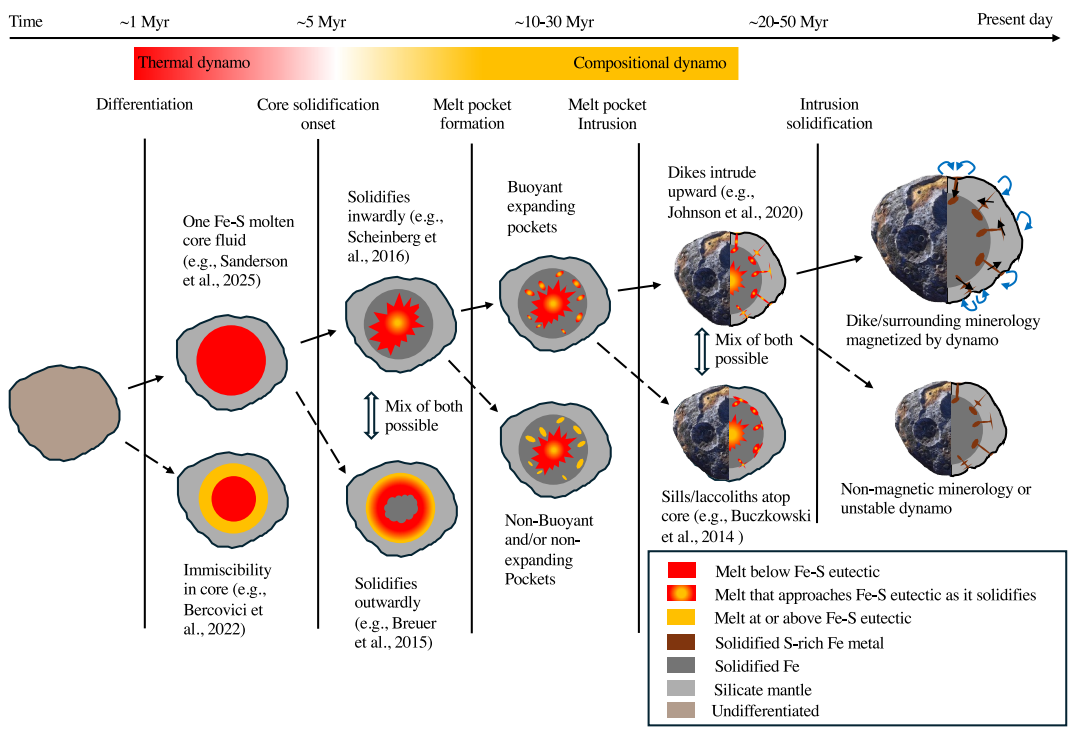

Figure 8. Summary timeline of events that could occur during core solidification on (16) Psyche. Solid arrows point toward the necessary evolution steps to produce magnetized ferromagmatic intrusions on the asteroid (16) Psyche. Dashed arrows lead to outcomes that would likely prohibit magnetized ferromagmatic intrusions.

(e.g., Soldati et al., 2021), clues could still be visible on Psyche's surface. The Psyche spacecraft's imager will map mineralogy with a spatial resolution of better than 500 m per pixel (Bell et al., 2025). Crucially, the multispectral imager investigation can reveal the presence of sulfide phases (Bell et al., 2025), like troilite (FeS), which would be a key diagnostic of ferrovolcanism. When combined with spectrally derived mineralogy, image derived topography can determine whether compositional heterogeneity is associated with impact depressions or other geomorphic structures. Complementing the imager derived mineralogy, the spacecraft's gamma ray and neutron spectrometer (GNRS) will quantify the abundances of Fe, Ni, and S with a minimum detection threshold of 4 wt. % (3 wt. % for S, Lawrence et al., 2025). The GRNS investigation will have a ∼70–110 km spatial resolution at the mission's closest orbit (Lawrence et al., 2025), approximately the size of the putative metal-rich regions identified on Psyche from ground-based observations (Cambioni et al., 2022). Finally, the gravity investigation will determine if mass is concentrated toward Psyche's interior, the case that would be expected if Psyche is a differentiated planetesimal (Zuber et al., 2022). Additionally, if Psyche solidified inwardly, then Psyche's moment of inertia should be greater than if Psyche solidified outwardly (Nichols-Fleming et al., 2024). These investigations, combined, will provide the necessary constraints to determine if Psyche had ferrovolcanism.

Consider the scenario where impacts have exposed ferromagmatic dikes and/or sills. In this case, there may be a region of impact-strewn metal. Iron depleted mantle silicates surround this region, exhibiting heterogeneity in the distribution of Fe, Ni, and S that the Psyche mission's GNRS could observe. The imager could identify finer scale heterogeneity, perhaps even identifying pure metal if there are exposures or boulders larger than the imager's resolution. However, these observations would not independently indicate ferromagmatism because an exposure of the top of the metal core itself, rather than the mantle-intruded metal, by impacts could exhibit a similar composition. In such a case, we argue that the detection of localized remanent magnetization could favor a ferromagmatism interpretation (see Section 5.3). In either case, Psyche would be differentiated, with mass radially concentrated toward its center. If the mission's gravity investigation determines that this is not the case, then ferromagmatism could be ruled-out, and other interpretations, such as a rubble pile or an undifferentiated body, would be more likely. Thus, we argue that the most conclusive evidence for ferromagmatism would be if Psyche appears differentiated and exhibits localized remanent magnetization correlated with evidence of sulfur-rich iron metal (at scales perhaps greater than imager resolution) exposed by impacts.

5.3. Crustal Remanent Magnetization Versus Dike Remanent Magnetization

Dikes provide the possibility of large volumes of material being magnetized quickly, and thus preserving a large uniform snapshot of the dynamo field. In contrast, the cooling crust could acquire remanent magnetization too, but on a much slower timescale. If undisturbed by impacts, the crust cools at a rate of ∼1 K per 1,000 years (Figure 5). Because we expect dynamos to vary in direction and amplitude on the order of kyrs (Neufeld et al., 2019), the crust would not acquire uniform magnetization. Remanence would vary in direction on a scale of meters. Non-uniform magnetization on this scale would be readily detectable in a hand sample but not by a spacecraft orbiting 75 km away. However, impacts could locally change the rate of cooling, so it may be possible that impacts could produce large detectable remanences, unrelated to ferromagmatic intrusions, which deserves further study.

In principle, an asteroidal material could acquire magnetization from an exogenous magnetic field, such as the solar wind or the solar nebular field (S. W. Courville et al., 2022; Oran et al., 2018). However, the solar wind likely could not have uniformally magnetized ferromagmatic intrusions because the intrusions would cool much too slowly compared to time variation of the solar wind, which is on the order of hours (Oran et al., 2018). Alternatively, although the solar nebular field would have provided a stronger and more stable magnetizing field that could impart uniform magnitization, the solar nebula dissipated by ∼5 Myrs after CAIs (Wang et al., 2017), which is long before ferromagmatic dikes would solidify. So the solar nebular magnetic field could not have magnetized ferromagmatic dikes or intrusions. Thus, we argue that ferromagmatic intrusions could only acquire magnetization from a long-lasting internal dynamo.

5.4. The Role of Impacts

We have focused on the magnetic signatures of ferromagmatism because impacts would likely have obliterated any Gyr-old surface features that may have been on Psyche's surface (Shepard et al., 2021). Because ferrovolcanic

eruptions would take place early in Psyche's history, we expect that flows of sulfur-rich melt that effused on the surface (Soldati et al., 2021), if they ever occurred, would have long been erased. For example, no volcanic features were observed on Vesta (D. A. Williams et al., 2014). However, that does not mean that all evidence of ferrovolcanism on the surface would have been erased. The remnants of iron and sulfur could still be deposited in patches across the surface, as suggested by the metal-rich regions seen by ALMA (Cambioni et al., 2022). Large impacts may have excavated ferromagmatic dikes or sills, dispersing their material over the broader surface of Psyche.

We focus on driving ferrovolcanism by sulfur enrichment in a spherically symmetric inwardly solidifying core. However, Psyche is not a sphere and almost certainly has been shaped by large impacts. Excavating material from the surface by impacts would break the assumed spherical symmetry of our thermal evolution and dynamo generation model. This could result in regions with faster mantle cooling and larger CMB heat flux. This rapid and heterogeneous cooling may strengthen the dynamo and alter the geometry of the magnetic field and should be investigated in the future. Much of the ferrovolcanism hypothesis relies on the conditions favorable to allow the negatively buoyant metal to intrude upward into the mantle. Excess pressure must be present to push the fluid upward. A large impact which excavates material could trigger fracturing (Abrahams & Nimmo, 2019) and reduce the excess pressure required to push material to the surface. Impacts may also expose ferrovolcanic dikes that do not reach the surface.

5.5. Broader Implications

If ferrovolcanism occurred on Psyche, then it is likely that the process may have occurred on other planetesimals that differentiated and experienced some degree of impact related mantle stripping. Ferrovolcanism could represent a process that would be a natural result of the average heating and impact rates on objects in the early solar system. Alternatively, ferrovolcanism could be a rather unique process to Psyche, having only been enabled by a specific set of impacts that stripped off most of the crust and mantle. Indeed, it is unlikely that ferrovolcanism could have been exposed to asteroids where crust/mantle removal did not occur. Regardless, if it were to occur on any celestial body, its effects would be important. By transporting metallic material from the core to the surface, ferrovolcanism could impact planetesimal core and mantle compositions, and hence, final planetary compositions. This mechanism could help explain the low sulfur contents of iron meteorites (Bercovici et al., 2022) and co-existence of metal and olivine in pallasite meteorites (Johnson et al., 2020). Detecting ferromagmatism at Psyche would shed light on a significant new process in planetesimal core evolution in the early Solar System.

6. Conclusion

The Psyche mission is well-equipped to look for signatures of ferrovolcanism on the asteroid (16) Psyche. However, obvious geomorphic evidence of ferrovolcanism, flows of molten sulfur-rich iron metal onto the surface, are not likely to have been preserved throughout Psyche's 4 Gyr history of impacts. We argue that the best chance of identifying ferrovolcanic features would be the observation of localized regions of sulfur-rich metal exposed or mixed with regolith on Psyche's surface, combined with spatially correlated magnetic field signatures. We demonstrate that ferromagmatic dikes could acquire remanent magnetization during their intrusion and that dikes more than ∼1 km wide could be detected by Psyche's magnetometer. However, we also identify several key requirements for ferrovolcanism, which are currently unconstrained: core fluid immiscibility driven by high abundances of sulfur and other light elements; dendritic core growth entrapping melt and generating a dynamo; and favorable fracture conduits to deliver the dense fluid against gravity through the less dense mantle. Therefore, the detection of magnetized ferromagmatic intrusions would place strong constraints on Psyche's formation history, requiring that the asteroid formed a core of a composition conducive to ferromagmatism and that the core solidified inwardly while generating a core dynamo.

Data Availability Statement

The thermal and dynamo evolution model data and ferromagmatism modelling that comprise the figures in this paper are freely available on GitHub (S. Courville, 2025). The thermal evolution and dynamo generation code that generated the thermal model data is freely available on GitHub (H. Sanderson, 2024).

Acknowledgments
This work was supported by NASA contract NNM16AA09, "Psyche: Journey to a Metal World. HRS acknowledges funding on a NERC studentship NE/S007474/1 and an Exonian Graduate Scholarship from Exeter College, University of Oxford. We acknowledge Dr. Jim Bell and Dr. David Lawrence for helpful discussions.

References

Abrahams, J. N. H., & Nimmo, F. (2019). Ferrovolcanism: Iron volcanism on metallic asteroids. *Geophysical Research Letters*, *46*(10), 5055–5064. https://doi.org/10.1029/2019GL082542

Annen, C. (2017). Factors affecting the thickness of thermal aureoles. *Frontiers in Earth Science*, *5*. https://doi.org/10.3389/feart.2017.00082

Bell, J. F., Ravine, M. A., Caplinger, M. A., Schaffner, J. A., Brylow, S. M., Clark, M. J., et al. (2025). The Psyche multispectral imager investigation: Characterizing the geology, topography, and multispectral properties of a metal-rich world. *Space Science Reviews*, *221*(4), 47. https://doi.org/10.1007/s11214-025-01169-3

Bercovici, H. L., Elkins-Tanton, L. T., O'Rourke, J. G., & Schaefer, L. (2022). The effects of bulk composition on planetesimal core sulfur content and size. *Icarus*, *380*, 114976. https://doi.org/10.1016/j.icarus.2022.114976

Berndt, T. A., Chang, L., Wang, S., & Badejo, S. (2018). Time-asymmetric FORC diagrams: A new protocol for visualizing thermal fluctuations and distinguishing magnetic mineral mixtures. *Geochemistry, Geophysics, Geosystems*, *19*(9), 3056–3070. https://doi.org/10.1029/2018gc007669

Bierson, C. J., Courville, S. W., Ermakov, A., Elkins-Tanton, L. T., Wieczorek, M., Park, R. S., & Baijal, N. (2025). (16) Psyche's different possible formation scenarios and internal structures from current constraints. *Journal of Geophysical Research: Planets*, *130*(4). https://doi.org/10.1029/2024je008640

Blakely, R. J. (1996). *Potential theory in gravity and magnetic applications*. Cambridge University Press.

Breuer, D., Rueckriemen, T., & Spohn, T. (2015). Iron snow, crystal floats, and inner-core growth: Modes of core solidification and implications for dynamos in terrestrial planets and moons. *Progress in Earth and Planetary Science*, *2*(1), 1–26. https://doi.org/10.1186/S40645-015-0069-Y

Brookfield, A., Cassidy, M., Weber, G., Popa, R.-G., Bachmann, O., & Stock, M. J. (2023). Magmatic volatile content and the overpressure "sweet spot": Implications for volcanic eruption triggering and style. *Journal of Volcanology and Geothermal Research*, *444*, 107916. https://doi.org/10.1016/j.jvolgeores.2023.107916

Buczkowski, D. L., Wyrick, D. Y., Toplis, M., Yingst, R. A., Williams, D. A., Garry, W. B., et al. (2014). The unique geomorphology and physical properties of the Vestalia Terra plateau. *Icarus*, *244*, 89–103. https://doi.org/10.1016/j.icarus.2014.03.035

Buono, A. S., & Walker, D. (2011). The Fe-rich liquidus in the Fe–FeS system from 1bar to 10GPa. *Geochimica et Cosmochimica Acta*, *75*(8), 2072–2087. https://doi.org/10.1016/j.gca.2011.01.030

Caldwell, W. K., Hunter, A., Plesko, C. S., & Wirkus, S. (2020). Understanding Asteroid 16 Psyche's composition through 3D impact crater modeling. *Icarus*, *351*, 113962. https://doi.org/10.1016/j.icarus.2020.113962

Cambioni, S., De Kleer, K., & Shepard, M. (2022). The heterogeneous surface of Asteroid (16) Psyche. *Journal of Geophysical Research: Planets*, *127*, e2021JE007091. https://doi.org/10.1029/2021JE007091

Chabot, N. L., & Drake, M. J. (2000). Crystallization of magmatic iron meteorites: The effects of phosphorus and liquid immiscibility. *Meteoritics & Planetary Sciences*, *35*(4), 807–816. https://doi.org/10.1111/j.1945-5100.2000.tb01464.x

Chabot, N. L., & Zhang, B. (2022). A revised trapped melt model for iron meteorites applied to the IIIAB group. *Meteoritics & Planetary Sciences*, *57*(2), 200–227. https://doi.org/10.1111/maps.13740

Clavé, E., Maurel, C., Lima, E. A., Shah, J., Mansbach, E. N., Uehara, M., & Weiss, B. P. (2020). A portable magnetometer for magnetic measurements of meter-sized meteorites. *Geochemistry, Geophysics, Geosystems*, *21*(11), e2020GC009266. https://doi.org/10.1029/2020GC009266

Clenet, H., Jutzi, M., Barrat, J.-A., Asphaug, E. I., Benz, W., & Gillet, P. (2014). A deep crust–mantle boundary in the asteroid 4 Vesta. *Nature*, *511*(7509), 303–306. https://doi.org/10.1038/nature13499

Consolmagno, G. J., Britt, D. T., & Macke, R. J. (2008). The significance of meteorite density and porosity. *Geochemistry*, *68*(1), 1–29. https://doi.org/10.1016/j.chemer.2008.01.003

Cournede, C., Gattacceca, J., Gounelle, M., Rochette, P., Weiss, B. P., & Zanda, B. (2015). An early solar system magnetic field recorded in CM chondrites. *Earth and Planetary Science Letters*, *410*, 62–74. https://doi.org/10.1016/j.epsl.2014.11.019

Courville, S. (2025). Ferromagmatism models. [Computational Notebook, Dataset]. *Zenodo*. https://doi.org/10.5281/zenodo.15571554

Courville, S. W., O'Rourke, J. G., Castillo-Rogez, J. C., Fu, R. R., Oran, R., Weiss, B. P., & Elkins-Tanton, L. T. (2022). Acquisition and preservation of remanent magnetization in carbonaceous asteroids. *Nature Astronomy*, *6*(12), 1387–1397. https://doi.org/10.1038/s41550-022-01802-z

De Kleer, K., Cambioni, S., & Shepard, M. (2021). The surface of (16) Psyche from thermal emission and polarization mapping. *Planetary Science Journal*, *2*(4), 149. https://doi.org/10.3847/PSJ/ac01ec

Dibb, S. D., Asphaug, E., Bell, J. F., Binzel, R. P., Bottke, W. F., Cambioni, S., et al. (2024). A post-launch summary of the science of NASA's Psyche mission. *AGU Advances*, *5*(Issue 2). https://doi.org/10.1029/2023AV001077

Dodds, K. H., Bryson, J. F. J., Neufeld, J. A., & Harrison, R. J. (2025). The direction of core solidification in asteroids: Implications for dynamo generation. *Icarus*, *425*, 116319. https://doi.org/10.1016/j.icarus.2024.116319

Elkins-Tanton, L. T., Asphaug, E., Bell, J. F., Bercovici, H., Bills, B., Binzel, R., et al. (2020). Observations, meteorites, and models: A preflight assessment of the composition and formation of (16) Psyche. *Journal of Geophysical Research: Planets*, *125*(3), 1–23. https://doi.org/10.1029/2019JE006296

Elkins-Tanton, L. T., Asphaug, E., Bell, J. F., Bierson, C. J., Bills, B. G., Bottke, W. F., et al. (2022). Distinguishing the origin of asteroid (16) Psyche. *Space Science Reviews*, *218*(3), 17. https://doi.org/10.1007/s11214-022-00880-9

Ermakov, A. I., Zuber, M. T., Smith, D. E., Raymond, C. A., Balmino, G., Fu, R. R., & Ivanov, B. A. (2014). Constraints on Vesta's interior structure using gravity and shape models from the Dawn mission. *Icarus*, *240*, 146–160. https://doi.org/10.1016/j.icarus.2014.05.015

Fagents, S. A., Lopes, R. M. C., Quick, L. C., & Gregg, T. K. P. (2022). 5—Cryovolcanism. In T. K. P. Gregg, R. M. C. Lopes, & S. A. Fagents (Eds.), *Planetary Volcanism Across the Solar System* (Vol. 1, pp. 161–234). Elsevier. https://doi.org/10.1016/B978-0-12-813987-5.00005-5

Farnocchia, D., Fuentes-Muñoz, O., Park, R. S., Baer, J., & Chesley, S. R. (2024). Mass, density, and radius of asteroid (16) Psyche from high-precision astrometry. *The Astronomical Journal*, *168*(1), 21. https://doi.org/10.3847/1538-3881/ad50ca

Ferreira, L. C., Stanton, N., Gordon, A. C., & Schmitt, R. (2023). The magmatic rifting of Santos basin: Aeromagnetic mapping of dykes, terranes and marginal structures and the interplay between tectonism and volcanism. *Tectonics*, *42*(4), e2022TC007560. https://doi.org/10.1029/2022TC007560

Fleet, M. E. (2006). Phase equilibria at high temperatures. *Reviews in Mineralogy and Geochemistry*, *61*(1), 365–419. https://doi.org/10.2138/rmg.2006.61.7

Flynn, G. J., Consolmagno, G. J., Brown, P., & Macke, R. J. (2018). Physical properties of the stone meteorites: Implications for the properties of their parent bodies. *Geochemistry*, *78*(3), 269–298. https://doi.org/10.1016/j.chemer.2017.04.002

Fu, R. R., Volk, M. W. R., Bilardello, D., Libourel, G., Lesur, G. R. J., & Ben Dor, O. (2021). The fine-scale magnetic history of the Allende Meteorite: Implications for the structure of the solar nebula. *AGU Advances*, *2*(3), e2021AV000486. https://doi.org/10.1029/2021AV000486

Goldstein, J. I., Scott, E. R. D., & Chabot, N. L. (2009). Iron meteorites: Crystallization, thermal history, parent bodies, and origin. *Chemie der Erde*, *69*(4), 293–325. https://doi.org/10.1016/j.chemer.2009.01.002

Gubbins, D. (1977). Energetics of the Earth's core. *Journal of Geophysics*, *43*(1), 453–464.

Hirschmann, M. M., Bergin, E. A., Blake, G. A., Ciesla, F. J., & Li, J. (2022). Early volatile depletion on planetesimals inferred from C-S systematics of iron meteorite parent bodies. *Proceedings of the National Academy of Sciences of the United States of America*, *118*(13), e2026779118. https://doi.org/10.1073/pnas.2026779118

Jaeger, J. C. (1964). Thermal effects of intrusions. *Reviews of Geophysics*, *2*(3), 443–466. https://doi.org/10.1029/RG002i003p00443

Johnson, B. C., Sori, M. M., & Evans, A. J. (2020). Ferrovolcanism on metal worlds and the origin of pallasites. *Nature Astronomy*, *4*(Issue 1), 41–44. https://doi.org/10.1038/s41550-019-0885-x

Kim, Y., & Hirabayashi, M. (2022). A numerical approach using a finite element model to constrain the possible interior layout of (16) Psyche. *Planetary Science Journal*, *3*(5), 122. https://doi.org/10.3847/PSJ/ac6b39

Lawrence, D. J., Goldsten, J. O., Peplowski, P. N., Burks, M. T., Cheng, S., Cully, M. J., et al. (2025). The Psyche gamma-ray and neutron spectrometer. *Space Science Reviews*.

Malvin, D. J., Jones, J. H., & Drake, M. J. (1986). Experimental investigations of trace element fractionation in iron meteorites. III: Elemental partitioning in the system Fe-Ni-S-P. *Geochimica et Cosmochimica Acta*, *50*(6), 1221–1231. https://doi.org/10.1016/0016-7037(86)90405-9

Maurel, C., Clavé, E., Gattacecca, J., Uehara, M., Mansbach, E. N., McCoy, T. J., & Weiss, B. P. (2025). Magnetization of iron meteorites up to the meter in size as possible analogs for asteroid Psyche. *Journal of Geophysical Research: Planets*, *130*(4), e2024JE008810. https://doi.org/10.1029/2024JE008810

Maurel, C., Weiss, B. P., & Bryson, J. F. J. (2019). Meteorite cloudy zone formation as a quantitative indicator of paleomagnetic field intensities and cooling rates on planetesimals. *Earth and Planetary Science Letters*, *513*, 166–175. https://doi.org/10.1016/j.epsl.2019.02.027

Morard, G., Bouchet, J., Rivoldini, A., Antonangeli, D., Roberge, M., Boulard, E., et al. (2018). Liquid properties in the Fe-FeS system under moderate pressure: Tool box to model small planetary cores. *American Mineralogist*, *103*(11), 1770–1779. https://doi.org/10.2138/am-2018-6405

Morard, G., & Katsura, T. (2010). Pressure-temperature cartography of Fe-S-Si immiscible system. *Geochimica et Cosmochimica Acta*, *74*(12), 3659–3667. https://doi.org/10.1016/j.gca.2010.03.025

Neufeld, J. A., Bryson, J. F. J., & Nimmo, F. (2019). The top-down solidification of iron asteroids driving dynamo evolution. *Journal of Geophysical Research: Planets*, *124*(5), 1331–1356. https://doi.org/10.1029/2018JE005900

Nichols, C. I. O., Bryson, J. F. J., Cottrell, R. D., Fu, R. R., Harrison, R. J., Herrero-Albillos, J., et al. (2021). A time-resolved paleomagnetic record of main group pallasites: Evidence for a large-cored, thin-mantled parent body. *Journal of Geophysical Research: Planets*, *126*(7). https://doi.org/10.1029/2021JE006900

Nichols-Fleming, F., Evans, A. J., Johnson, B. C., & Sori, M. M. (2022). Porosity evolution in metallic asteroids: Implications for the origin and thermal history of asteroid 16 Psyche. *Journal of Geophysical Research: Planets*, *127*(2), e2021JE007063. https://doi.org/10.1029/2021JE007063

Nichols-Fleming, F., Evans, A. J., Johnson, B. C., & Sori, M. M. (2024). Moment of inertia and tectonic record of asteroid 16 Psyche may reveal interior structure and core solidification processes. *Journal of Geophysical Research: Planets*, *129*(7), e2024JE008291. https://doi.org/10.1029/2024JE008291

Nimmo, F. (2007). Energetics of the core. In *Treatise on geophysics* (1st ed., Vol. 8, pp. 33–62). Elsevier. https://doi.org/10.1016/b978-044452748-6.00128-0

O'Brien, T., Tarduno, J. A., Anand, A., Smirnov, A. V., Blackman, E. G., Carroll-Nellenback, J., & Krot, A. N. (2020). Arrival and magnetization of carbonaceous chondrites in the asteroid belt before 4562 million years ago. *Communications Earth & Environment*, *1*(1), 54. https://doi.org/10.1038/s43247-020-00055-w

Oran, R., Weiss, B. P., & Cohen, O. (2018). Were chondrites magnetized by the early solar wind? *Earth and Planetary Science Letters*, *492*, 222–231. https://doi.org/10.1016/j.epsl.2018.02.013

Raghavan, V. (1987). Phase diagrams of ternary iron alloys. (No Title).

Rückriemen, T., Breuer, D., & Spohn, T. (2015). The Fe snow regime in Ganymede's core: A deep-seated dynamo below a stable snow zone. *Journal of Geophysical Research: Planets*, *120*(6), 1095–1118. https://doi.org/10.1002/2014JE004781

Sanderson, H. (2024). A refined, versatile model for planetesimal thermal evolution and dynamo generation (1.0.0) [Software]. https://doi.org/10.5281/zenodo.12771396

Sanderson, H. R., Bryson, J. F. J., Nichols, C. I. O., & Davies, C. J. (2025). Unlocking planetesimal magnetic field histories: A refined, versatile model for thermal evolution and dynamo generation. *Icarus*, *425*, 116323. https://doi.org/10.1016/j.icarus.2024.116323

Sanderson, H. R., Bryson, J. F. J., & Nichols, C. I. O. (2024). Early and elongated epochs of planetesimal dynamo generation. *Earth and Planetary Science Letters*, *648*, 119083. https://doi.org/10.1016/j.epsl.2024.119083

Scheinberg, A., Elkins-Tanton, L. T., Schubert, G., & Bercovici, D. (2016). Core solidification and dynamo evolution in a mantle-stripped planetesimal. *Journal of Geophysical Research: Planets*, *121*(1), 2–20. https://doi.org/10.1002/2015JE004843

Shepard, M. K., Kleer, K. D., Cambioni, S., Taylor, P. A., Virkki, A. K., Rívera-Valentin, E. G., et al. (2021). Asteroid 16 Psyche: Shape, features, and global map. *Planetary Science Journal*, *2*(4), 125. https://doi.org/10.3847/PSJ/abfdba

Siltala, L., & Granvik, M. (2021). Mass and density of asteroid (16) Psyche. *The Astrophysical Journal Letters*, *909*(1), L14. https://doi.org/10.3847/2041-8213/abe948

Soldati, A., Farrell, J. A., Wysocki, R., & Karson, J. A. (2021). Imagining and constraining ferrovolcanic eruptions and landscapes through large-scale experiments. *Nature Communications*, *12*(1), 1711. https://doi.org/10.1038/s41467-021-21582-w

Tarduno, J. A., Cottrell, R. D., Nimmo, F., Hopkins, J., Voronov, J., Erickson, A., et al. (2012). Evidence for a dynamo in the main group pallasite parent body. *Science*, *338*(6109), 939–942. https://doi.org/10.1126/science.1223932

Tauxe, L. (2010). *Essentials of paleomagnetism*. University of California press.

Turcotte, D. L., & Schubert, G. (2002). *Geodynamics*. Cambridge University Press.

Ulff-Moller, F. (1998). Effects of liquid immiscibility on trace element fractionation in magmatic iron meteorites: A case study of group IIIAB. *Meteoritics & Planetary Sciences*, *33*(2), 207–220. https://doi.org/10.1111/j.1945-5100.1998.tb01626.x

Wang, H., Weiss, B. P., Bai, X.-N., Downey, B. G., Wang, J., Wang, J., et al. (2017). Lifetime of the solar nebula constrained by meteorite paleomagnetism. *Science*, *355*(6325), 623–627. https://doi.org/10.1126/science.aaf5043

Watanabe, M., Adachi, M., & Fukuyama, H. (2016). Densities of Fe–Ni melts and thermodynamic correlations. *Journal of Materials Science*, *51*(7), 3303–3310. https://doi.org/10.1007/s10853-015-9644-2

Watters, T. R., Robinson, M. S., Bina, C. R., & Spudis, P. D. (2004). Thrust faults and the global contraction of Mercury. *Geophysical Research Letters*, *31*(4). https://doi.org/10.1029/2003GL019171

Weiss, B. P., Merayo, J. M. G., Ream, J. B., Oran, R., Brauer, P., Cochrane, C. J., et al. (2023). The Psyche magnetometry investigation. *Space Science Reviews*, *219*(3), 22. https://doi.org/10.1007/s11214-023-00965-z

Williams, D. A., O'Brien, D. P., Schenk, P. M., Denevi, B. W., Carsenty, U., Marchi, S., et al. (2014). Lobate and flow-like features on asteroid Vesta. *Planetary and Space Science*, *103*, 24–35. https://doi.org/10.1016/j.pss.2013.06.017

Williams, Q. (2009). Bottom-up versus top-down solidification of the cores of small solar system bodies: Constraints on paradoxical cores. *Earth and Planetary Science Letters*, *284*(3–4), 564–569. https://doi.org/10.1016/J.EPSL.2009.05.019

Williams, Q. (2025). A note on the direction of core solidification in asteroids, the iron melting curve, and phase equilibria parameterizations. *Icarus*, *427*, 116381. https://doi.org/10.1016/j.icarus.2024.116381

Wilson, L., & Keil, K. (2012). Volcanic activity on differentiated asteroids: A review and analysis. *Geochemistry*, *72*(4), 289–321. https://doi.org/10.1016/j.chemer.2012.09.002

Zhang, F., Pizzi, A., Ruj, T., Komatsu, G., Yin, A., Dang, Y., et al. (2023). Evidence for structural control of mare volcanism in lunar compressional tectonic settings. *Nature Communications*, *14*(1), 2892. https://doi.org/10.1038/s41467-023-38615-1

Zuber, M. T., Park, R. S., Elkins-Tanton, L. T., Bell, J. F., Bruvold, K. N., Bercovici, D., et al. (2022). The Psyche gravity investigation. *Space Science Reviews*, *218*(8), 57. https://doi.org/10.1007/s11214-022-00905-3